

1 Cumulative and individual impacts of the human 2 footprint on biodiversity indicators using dissimilarity 3 to high integrity reference states.

4 **Evan Muise¹, Nicholas Coops¹, Txomin Hermosilla², Chris Mulverhill¹, Cole
5 Burton¹, Stephen Ban³**

6 ¹Department of Forest Resource Management, University of British Columbia, Vancouver, British
7 Columbia, Canada,

8 ²Canadian Forest Service (Pacific Forestry Centre), Natural Resources Canada, Victoria, British
9 Columbia, Canada,

10 ³BC Parks, Government of British Columbia, Victoria, British Columbia, Canada,

11 **Abstract**

12 Forests with high ecological integrity are incredibly important for biodiversity
13 conservation, and provide integral ecosystem services. These forests have natural
14 or near-natural ecosystem structure, function, and composition. Anthropogenic
15 pressures such as habitat loss, overexploitation of natural resources, and land use
16 changes are leading to the degradation or loss of high-integrity forests. As a result,
17 assessing forest integrity over large areas is increasingly important for a range of
18 conservation initiatives. Recently, we have seen an increase in the application of
19 remote sensing data to assess a range of forest structural and functional attributes,
20 which can provide insights into forest integrity through space and time. In this
21 study, we use satellite-derived forest structural attributes and forest functioning
22 metrics alongside a high-quality reference state to calculate ecological dissimilarity
23 as a proxy for ecological integrity. We further refine our reference states by using
24 coarsened exact matching to ensure our comparisons are drawn from suitable pro-
25 tected analogs. We applied these methods onto Vancouver Island, Canada, where
26 we assessed how far, in structural and functional space, forest stands were from
27 reference, high-integrity forests found in the island's oldest and largest protected
28 area. We further assess how individual and cumulative anthropogenic pressure
29 are influencing the ecological integrity of forests on the island. We found that for-
30 est structural dissimilarity increased under high levels of anthropogenic pressures
31 (ANOVA; $p < 0.01$), while functional dissimilarity was not impacted by any an-
32 thropogenic pressures (ANOVA; $p > 0.05$). For individual pressures, we found that
33 built environments, harvesting, and population density influenced structural dis-
34 similarity (ANOVA; $p < 0.05$), while roads did not influence structural dissimilarity
35 (ANOVA; $p > 0.05$). These types of methods can be used to identify high-integrity
36 forest ecosystems which should be prioritized for protection, or to identify areas with
37 low levels of pressures which could benefit from restoration efforts, helping move
38 towards the Kunming-Montreal Global Biodiversity Framework's goal of 30% of all
39 ecosystems protected, with a focus on high-integrity ecosystems

40 **Introduction**

41 In the terrestrial environment, forests have been shown to possess large amounts
42 of biodiversity (Cardinale et al., 2012; Myers, 1988; Pimm and Raven, 2000) and
43 provide key ecosystem services (Thompson et al., 2009). However, the ongoing im-
44 pact of anthropogenic pressures such as climate change, overexploitation of natural
45 resources, and invasive species are leading to forest degradation, reducing the ability
46 of forested ecosystems to provide these services (Thomas et al., 2004; Urban, 2015).
47 Therefore it is integral to maintain and conserve forests that are in good ecological

Corresponding author: Evan Muise, evanmuise@student.ubc.ca

48 condition, as defined by natural or near-natural levels of forest structure, function,
 49 and composition, often referred to as having high ecological integrity (Marín et al.,
 50 2021). The importance of high-integrity ecosystems has led to a general call to move
 51 beyond simple quantification of ecosystem or forest extent in conservation strategies
 52 to other metrics which additionally consider the integrity of the conserved ecosystem
 53 (Ferrier et al., 2024; Hansen et al., 2020; Muise et al., 2022; Pillay et al., 2024a). In
 54 December 2022, the Kunming-Montreal Global Biodiversity Framework (GBF) was
 55 adopted with the goal of restoring and safeguarding global biodiversity (Convention
 56 on Biological Diversity, 2023). Targets within this framework include restoring 30%
 57 of all degraded ecosystems, protecting 30% of the Earth's terrestrial, inland water,
 58 and marine areas by 2030, and achieving no loss of high biodiversity importance
 59 areas, especially high ecological integrity ecosystems (Convention on Biological Di-
 60 versity, 2023). However, there are currently no spatially explicitly assessments of
 61 ecological integrity available at the regional or larger scale, making progress towards
 62 these goals difficult to quantify.

63 Assessing ecological integrity requires a comprehensive evaluation of ecosystem
 64 structure, function, and composition, which can be effectively achieved using re-
 65 mote sensing-derived indicators (Pereira et al., 2013; Radeloff et al., 2024; Skidmore
 66 et al., 2021). Advances in remote sensing technologies such as light detection and
 67 ranging (lidar) allow for the accurate measurement of forest structural attributes,
 68 including canopy height, canopy cover, vertical complexity, and biomass (Bergen
 69 et al., 2009; Valbuena et al., 2020). These indicators of forest structure can pro-
 70 vide critical insights into habitat quality and the capacity of ecosystems to support
 71 biodiversity (Gao et al., 2014; Guo et al., 2017; MacArthur and MacArthur, 1961),
 72 and are rapidly becoming available at the national scale through new modelling
 73 methods (Matasci et al., 2018a; Matasci et al., 2018b; Potapov et al., 2021). Addi-
 74 tionally, remote sensing facilitates the monitoring of functional processes, such as
 75 photosynthetic activity and forest phenology, through the use of spectral indices
 76 such as the normalized difference vegetation index (NDVI) (Pettorelli et al., 2018,
 77 2005), amongst others. By integrating these indices over the course of the year, it
 78 is possible to assess the energy availability, seasonality, and stress on an ecosystem
 79 (Radeloff et al., 2019; Razenkova, 2023), which have also been shown to be linked
 80 to biodiversity in a variety of taxa (Andrew et al., 2024, 2012; Coops et al., 2019,
 81 2009b; Razenkova et al., 2022). Further, structural and functional indicators have
 82 been shown to have low information overlap (Muise et al., 2024), thereby making it
 83 suitable use satellite-derived structural and functional indicators to assess ecolog-
 84 ical integrity across regions, countries, or even continents by comparing them to a
 85 suitable reference state (Grantham et al., 2020; Hansen et al., 2020).

86 Another key aspect of assessing ecological integrity is the reference state, typically
 87 defined as an example of an ecosystem that has not been subject major anthro-
 88 pogenic disturbance (Hansen et al., 2020; Nicholson et al., 2021). These reference
 89 states represent the baseline conditions of ecosystems and serve as a benchmark for
 90 assessing ecological health and guiding protection and restoration efforts (Nielsen
 91 et al., 2007). A number of methods have been proposed for identifying reference
 92 states, including protected areas (Arcese and Sinclair, 1997), historical (McNellie et
 93 al., 2020), and empirical reference states (Ferraro, 2009; Nielsen et al., 2007). Pro-
 94 tected area reference states are commonly used because conservation efforts aim to
 95 mitigate anthropogenic pressures within protected areas (Geldmann et al., 2019),
 96 and the bias for protected areas to be placed in areas with low amounts of anthro-
 97 pogenic pressures (Joppa and Pfaff, 2009) and less productive land covers (Muise et
 98 al., 2022). Due to the bias in protected area placement, it is necessary to account for
 99 differences in environmental conditions and land covers when using them as a refer-
 100 ence state, which is typically accomplished using counterfactual methods (Ferraro,
 101 2009), such as coarsened exact matching (Iacus et al., 2012). Using these methods

102 it becomes possible to identify a suitable reference state for the entirety of a re-
 103 gion, by comparing to protected areas without anthropogenic pressure under similar
 104 environmental conditions and land covers.

105 Building on this foundation, the objective of this study is to develop and imple-
 106 ment a spatially explicit framework for assessing ecological integrity at regional to
 107 continental scales using remote sensing data. Specifically, we aim to (1) integrate
 108 satellite-derived indicators of forest structure and function with robust counter-
 109 factual methods to establish reference states, (2) quantify deviations from these
 110 reference states as a measure of ecological degradation, and (3) demonstrate the
 111 utility of this method across a regional study area. This work addresses a critical
 112 gap in the operationalization of global biodiversity targets, such as those outlined in
 113 the GBF, by providing a scalable, reproducible approach to monitor and guide con-
 114 servation and restoration efforts. By enabling the identification of areas with high
 115 ecological integrity and those most in need of restoration, this study has the poten-
 116 tial to directly inform policy and support more effective biodiversity conservation
 117 strategies.

118 Methods

119 To accomplish our objectives, we propose a novel, data-driven approach to identify
 120 high-integrity forests based on various satellite derived metrics of ecosystem condi-
 121 tion. First, we account for differences in environmental conditions by implementing
 122 a coarsened exact matching approach (Iacus et al., 2012). This ensures that ecosys-
 123 tems must be similar to their protected counterparts (i.e. a forest in a valley bottom
 124 and a mountain top would not be compared to one another), which accounts for
 125 biases in protected area placement (Joppa and Pfaff, 2009; Muise et al., 2022). We
 126 use the sigma dissimilarity metric (Mahony et al., 2017) to calculate the similarity
 127 to high-integrity, undisturbed, forests in both structural and functional space as a
 128 metric of ecological integrity. Finally, we validate our results by assessing the im-
 129 pact anthropogenic pressures (Hirsh-Pearson et al., 2022) on our similarity metric,
 130 with the assumption that increased anthropogenic pressures should increase ecolog-
 131 ical dissimilarity. We focus our study area on Vancouver Island, British Columbia,
 132 Canada, as a case study and demonstration of the method.

133 Study Area

134 We focus on the forested areas of Vancouver Island, British Columbia, Canada. Van-
 135 couver Island has approximately 31,285 km² of land area, of which 79.5% is forested.
 136 The dominant forest species on Vancouver Island are Douglas-fir (*Pseudotsuga men-*
 137 *ziesii*), western red cedar (*Thuja plicata*), western hemlock (*Tsuga heterophylla*),
 138 yellow cedar (*Chamaecyparis nootkatensis*), and Sitka spruce (*Picea sitchensis*)
 139 (Burns, 1990). Vancouver Island generally has a temperate maritime climate, with
 140 mild, wet winters, and cool, dry summers. There are four ecosystems on Vancou-
 141 ver Island as defined by British Columbia's biogeoclimatic ecosystem classifica-
 142 tion (BEC) framework (Pojar et al., 1987), Coastal Western Hemlock (CWH), Mountain
 143 Hemlock (MH), Coastal Douglas Fir (CDF), and Coastal Mountain-heather Alpine
 144 (CMA), which are broadly delineated based on soil, climate, and elevation. Forestry
 145 is an important industry on Vancouver Island, with the majority of the land base
 146 being managed for timber production under various tenures, including private own-
 147 ership (Ministry of Water, Land and Resource Stewardship (WLRS), 2023). These
 148 harvesting practices have led to a need to protect remaining high-integrity forests,
 149 and restore degraded forests. Fires on Vancouver Island have historically been infre-
 150 quently and of low severity (Daniels and Gray, 2006).

151 Reference State

152 Strathcona Park provided an exceptional reference state for the undisturbed forest
 153 ecosystems on Vancouver Island due to its long-standing protection and large size.
 154 Established in 1911 as the oldest and largest provincial park in British Columbia, it

encompasses 2,480 km², with approximately 80% designated as wilderness and Nature Conservancy Areas under the Park Act (“Park Act,” 1996). These designations have ensured the preservation of natural ecological processes, leaving the park relatively free from anthropogenic disturbances over more than a century. Strathcona Park includes three of the island’s BEC zones: CWH, MH, and CMA. However, the CDF zone, limited to the southern part of Vancouver Island and subject to extensive anthropogenic alteration, is not represented within the park. As such, we do not include CDF in our analysis. By focusing on undisturbed forests within Strathcona Park as a reference state, our analysis prioritizes areas of minimal human impact and ecological continuity, providing a robust benchmark for assessing forest ecosystems in their natural state.

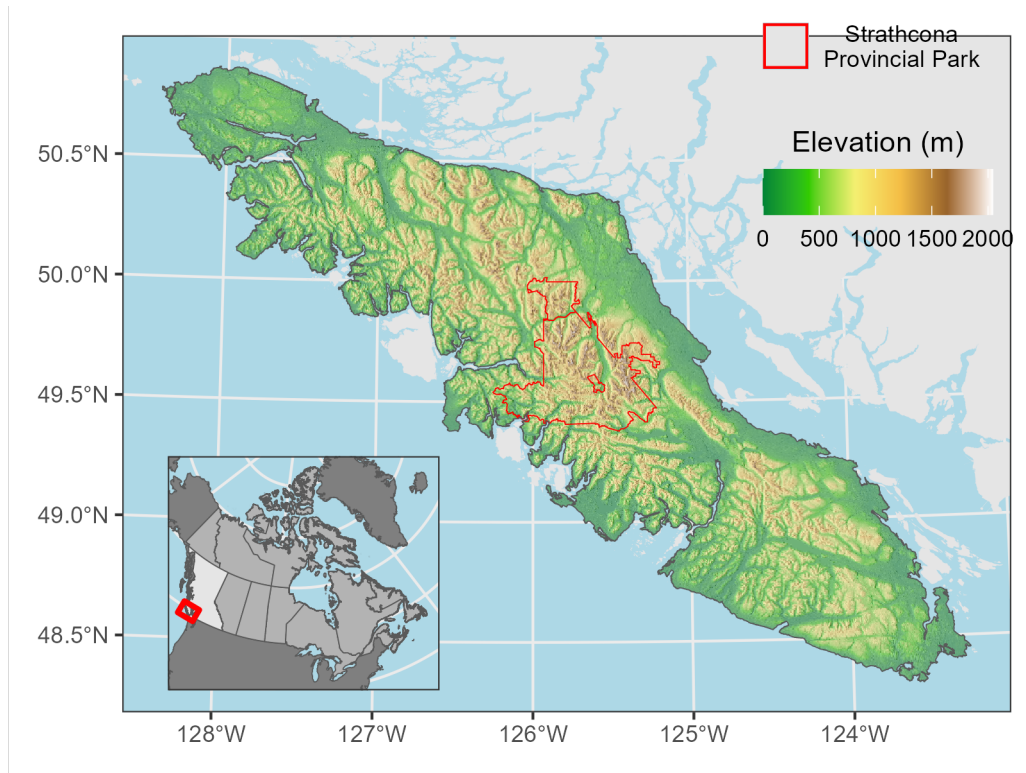


Figure 1: Study area on Vancouver Island, British Columbia, Canada, including the location of Strathcona Provincial Park.

166 Data

167 *Forest Structure*

168 We utilize four forest structural attributes; canopy height, canopy cover, structural
 169 complexity, and aboveground biomass. Canopy height, canopy cover, structural
 170 complexity are standardized lidar-derived metrics suitable for biodiversity moni-
 171 toring at the ecosystem scale (Valbuena et al., 2020). These are commonly used to
 172 assess patterns of structure in the vertical and horizontal directions within a single
 173 stand, rather than across a landscape, with these stand level metrics being linked
 174 to habitat, and thus, biodiversity (Bergen et al., 2009; Gao et al., 2014; Macarthur
 175 and Macarthur, 1961). The fourth attribute, aboveground biomass, represents the
 176 key ecosystem service of carbon sequestration (Duncanson et al., 2023; Naidoo and

177 Ricketts, 2006), and is likely moderated by the three lidar-derived variables (Ali,
 178 2019).

179 These four forest structural attributes were generated in a wall-to-wall fashion at a
 180 30 m spatial resolution by Matasci et al. (2018a) for the year 2015 using a random
 181 forest-kNN approach, that imputes lidar-derived forest structural attributes across
 182 Canada's forested ecosystems using Landsat-derived best-available-pixel (BAP) com-
 183 posites (Hermosilla et al., 2016; White et al., 2014) and topographic information
 184 (Matasci et al., 2018a; Matasci et al., 2018b). The BAP composites were gener-
 185 ated by selecting surface reflectance observations from the Landsat archive over the
 186 course of Canada's growing season (August 1st ± 30 days), avoiding atmospheric
 187 effects including haze, clouds, and cloud shadows. These composites were further re-
 188 fined by using a spectral trend analysis remove noise and infill data gaps (Hermosilla
 189 et al., 2015). Accuracy metrics for the forest structural attributes ranged from an
 190 RMSE of 29.7% (structural complexity) to 65.8% (aboveground biomass) and R²
 191 values of 0.70 (aboveground biomass) to 0.13 (structural complexity).

192 **Forest Function**

193 To represent forest ecosystem function, we use the Dynamic Habitat Indices (DHIs)
 194 dataset, a suite of intra-annual summaries of energy (as represented by a vegeta-
 195 tion index or estimate of gross/net primary productivity) availability (Radeloff et
 196 al., 2019). Single time points of energy availability have commonly been used as
 197 indicators of ecosystem functioning (Pettorelli et al., 2018, 2005), and the DHIs ad-
 198 vance upon these snapshots by generating yearly summaries of energy availability,
 199 thus more strongly linking these metrics to ecosystem functioning. The DHIs are
 200 composed of the total available energy over the course of a year (Cumulative DHI),
 201 the minimum amount of energy available over the course of a year (Minimum DHI),
 202 and the variation in energy available over the course of a year (Variation DHI). The
 203 DHIs have been shown to be indicative of ecosystem functioning, as they represent
 204 energy availability and seasonality (Berry et al., 2007), and biodiversity over a range
 205 of scales (Radeloff et al., 2019; Razenkova et al., 2022), extents (Coops et al., 2019,
 206 2009a) and taxa (Michaud et al., 2014; Suttidate et al., 2021).

207 We calculated the DHIs at a 30 m spatial resolution using Landsat data, following
 208 the methodology of Razenkova (2023). The DHIs were computed on Google Earth
 209 Engine (Gorelick et al., 2017) by creating a synthetic year of monthly NDVI com-
 210 posites using all available Landsat imagery from 2011-2020 (centred on 2015). We
 211 used the Landsat QA band (Zhu and Woodcock, 2012) to filter pixels with clouds
 212 and cloud shadows. Monthly NDVI values were calculated by taking the median of
 213 each month's NDVI observations, ignoring the year the image was acquired. This
 214 resulted in DHIs at 30 m spatial resolution (Razenkova, 2023). The DHIs are calcu-
 215 lated as the sum (Cumulative DHI), minimum (Minimum DHI), and coefficient of
 216 variation (Variation DHI) of these monthly observations. In this study, we focus on
 217 the Cumulative and Variation DHIs, as the minimum DHI is consistently 0 due to
 218 the presence of snow during winter in our study area.

219 **Anthropogenic Pressures**

220 We used the Canadian Human Footprint as developed by Hirsh-Pearson et al.
 221 (2022) to indicate anthropogenic pressures on the environment. The Canadian
 222 Human Footprint is an additive pressure map generated by summing the 12 different
 223 anthropogenic pressures (built environments, crop land, pasture land, population
 224 density, nighttime lights, railways, roads, navigable waterways, dams and associ-
 225 ated reservoirs, mining activity, oil and gas, and forestry), which ranges from zero
 226 to 55 for any cell across Canada. This cumulative dataset is also distributed with
 227 Canada-wide individual pressure values (Hirsh-Pearson et al., n.d.). We use the an-
 228 thropogenic pressure layers to define our reference state by excluding pixels with any
 229 amount of anthropogenic pressure in Strathcona Park, and also assess the impact of

anthropogenic pressures on ecological integrity. Here, we focus on the overall cumulative pressure map and four individual pressures: population density, built environments, roads, and forestry. We selected these four as other pressures (oil and gas; railroads) are not present on Vancouver Island, while pasture land and crop land do not coincide with currently forested areas. We reclassify the Canadian Human Footprint (Hirsh-Pearson et al., n.d.; Hirsh-Pearson et al., 2022) into categorical data following Hirsh-Pearson et al. (2022) and Arias-Patino et al. (2024): a value of zero is considered intact, zero to four has low anthropogenic pressure, four to eight has medium anthropogenic pressure, and above eight has high anthropogenic pressure.

Covariates

In order to ensure that we were identifying suitable reference states, we matched undisturbed forest areas within Strathcona Park with forested areas outside the park based on topographic and climatic features. We use a 30 m digital elevation model and derived slope dataset from the Advanced Spaceborne Thermal Emission and Reflection Radiometer (ASTER) Version 3 GDEM product (Abrams et al., 2020). We also used four climate variables; mean annual precipitation (MAP), mean annual temperature (MAT), mean warmest month temperature (MWMT), and mean coldest month temperature (MCMT) calculated from 1990-2020 climate normals using the ClimateNA software package at a 1 km spatial resolution, and downsampled to 30 m using cubic spline resampling in the **terra** (version 1.7-71) R package (Hijmans, 2024) in R (R Core Team, 2024 version 4.4.1). A visualization of one of each input dataset can be found in Figure 2.

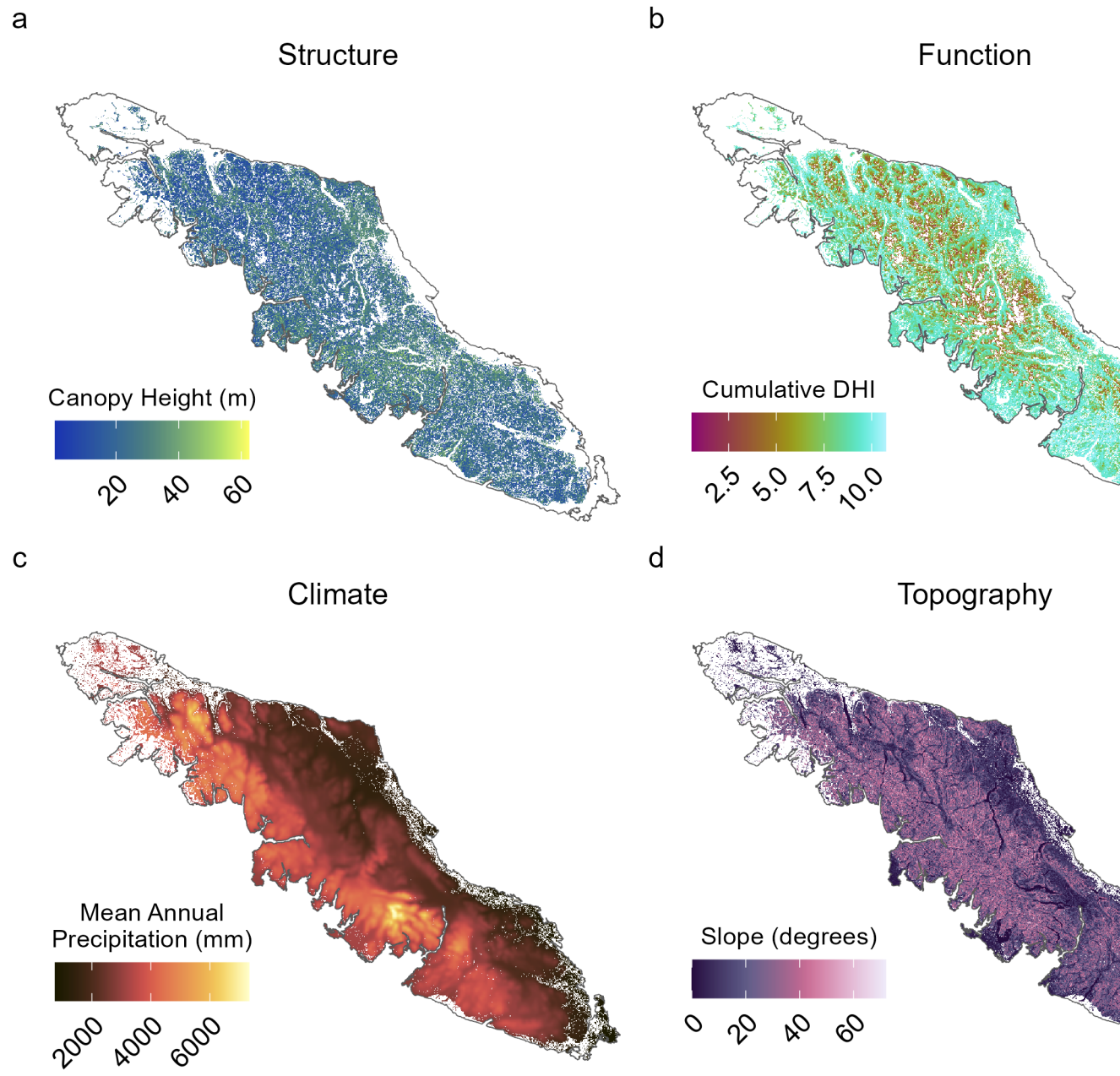


Figure 2: Examples of each of the four major datasets used in our study. Panels a and b show structure and function, respectively, used for the calculation of sigma dissimilarity. Panels c and d show climate and topography, respectively, used for the coarsened exact matching procedure.

252 **Calculating Ecological Dissimilarity**

253 We calculated the sigma dissimilarity (Mahony et al., 2017) of forested pixels across
 254 our study area by using an expanded coarsened exact matching (CEM) technique
 255 (Iacus et al., 2012) (Figure 3) for each forest type (broadleaf, coniferous, mixed
 256 wood, and wetland-treed) (Hermosilla et al., 2018). The CEM technique creates
 257 comparable groups of observations across covariates by initially coarsening the
 258 covariates. In this instance, all six covariates (elevation, slope, mean annual pre-
 259 precipitation, mean annual temperature, mean coldest month temperature, and mean
 260 warmest month temperature) were coarsened into five quintiles, hereafter referred to
 261 as bins. CEM then performs exact matching on the bins, with each pixel matched to
 262 a climatically and topographically similar group of pixels within the reference state
 263 (i.e. Strathcona Park), hereafter referred to as stratum. If insufficient numbers of
 264 matched pixels were found in the reference state, we calculated the stratum's nearest
 265 neighbour across covariate bins, and sampled up to 100 pixels, while minimizing the
 266 nearest neighbour distance. If the average nearest neighbour distance was greater
 267 than two, that stratum was excluded from the analysis.

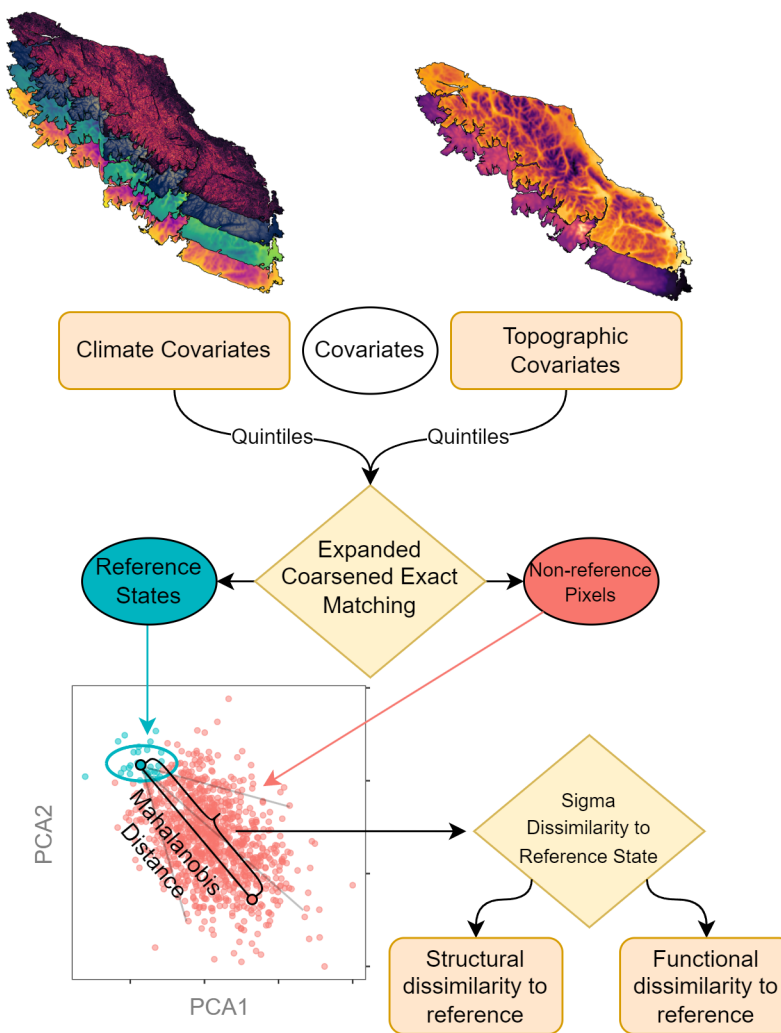


Figure 3: Conceptual flow diagram of the study.

Following the matching procedure, we identified reference states as undisturbed (human footprint = 0; no fire or harvesting disturbance) (Hermosilla et al., 2015; Hirsh-Pearson et al., 2022) pixels by stratum within Strathcona Park. We then determine the dissimilarity of all pixels, in structural, functional, and structural + functional attributes, to the reference states by calculating the sigma dissimilarity metric. Sigma dissimilarity standardizes the Mahalanobian distance (Mahalanobis, 1936) by rescaling it into percentiles of the chi distribution to account for the effect of dimensionality when creating a multivariate dissimilarity metric (Mahony et al., 2017). We calculated sigma dissimilarity for every stratum with a suitable reference state as generated by our matching procedure. This dissimilarity metric effectively functions as a multivariate proxy for ecological integrity, with higher values indicating a larger difference from near natural conditions found within the reference state.

Impacts of anthropogenic pressure on ecological dissimilarity

To assess the cumulative impact of anthropogenic pressure on ecological dissimilarity, we implement stratified sampling on all suitable stratum, sampling 100 samples from each anthropogenic pressure class. For our individual pressures, we sampled an additional 100 samples for each pressure class. Sampling was performed using the **sgsR** (version 1.4.5) R package (Goodbody et al., 2023) with the Quiennec method (Queinnec et al., 2021). Geospatial data processing was performed using the **terra** (version 1.7-78) (Hijmans, 2024), **sf** (version 1.0-16) (Pebesma, 2018; Pebesma and Bivand, 2023), and **tidyterra** (version 0.6.1) (Hernangómez, 2023) R packages.

We used a one-way analysis of variance (ANOVA) with a critical p value of 0.05 to identify statistically significant differences in the mean similarity values across cumulative anthropogenic pressure classes. We account for family-wise error rate in our ANOVAs using the Holm-Bonferroni method (Holm, 1979), only continuing the analysis for similarity variables with significant ANOVAs at the adjusted critical value. We used a Tukey HSD post-hoc test to identify which means are different from the control group (intact pixels), which also controls for the family-wise error rate.

We follow the same protocol to identify the difference in means for each anthropogenic pressure of interest (roads, population density, forestry, and built environment). We compare each pressure to the same ‘no pressure’ values sampled in the cumulative pressure analysis. All statistical analysis were conducted using the **rstatix** (version 0.7.2) R package (Kassambara, 2023).

Results

We generated maps of sigma dissimilarity for ecosystem structure, function, and structure + function across Vancouver Island as a measure of ecological integrity (Figure 4). We show three representative examples within Vancouver Island to display the impact of anthropogenic pressures on ecosystem similarity, displaying a region near Lake Cowichan where harvesting is a common pressure (Figure 4 A), a protected area (Elk Falls Provincial Park) near Campbell River with high population density (Figure 4 B), and a region with lower anthropogenic pressures (Figure 4 C). Functional dissimilarity shows higher variation across all three sites than functional or structural and functional dissimilarity. The protected region near Campbell River (Figure 4 B) has lower dissimilarity metrics for all three metrics.

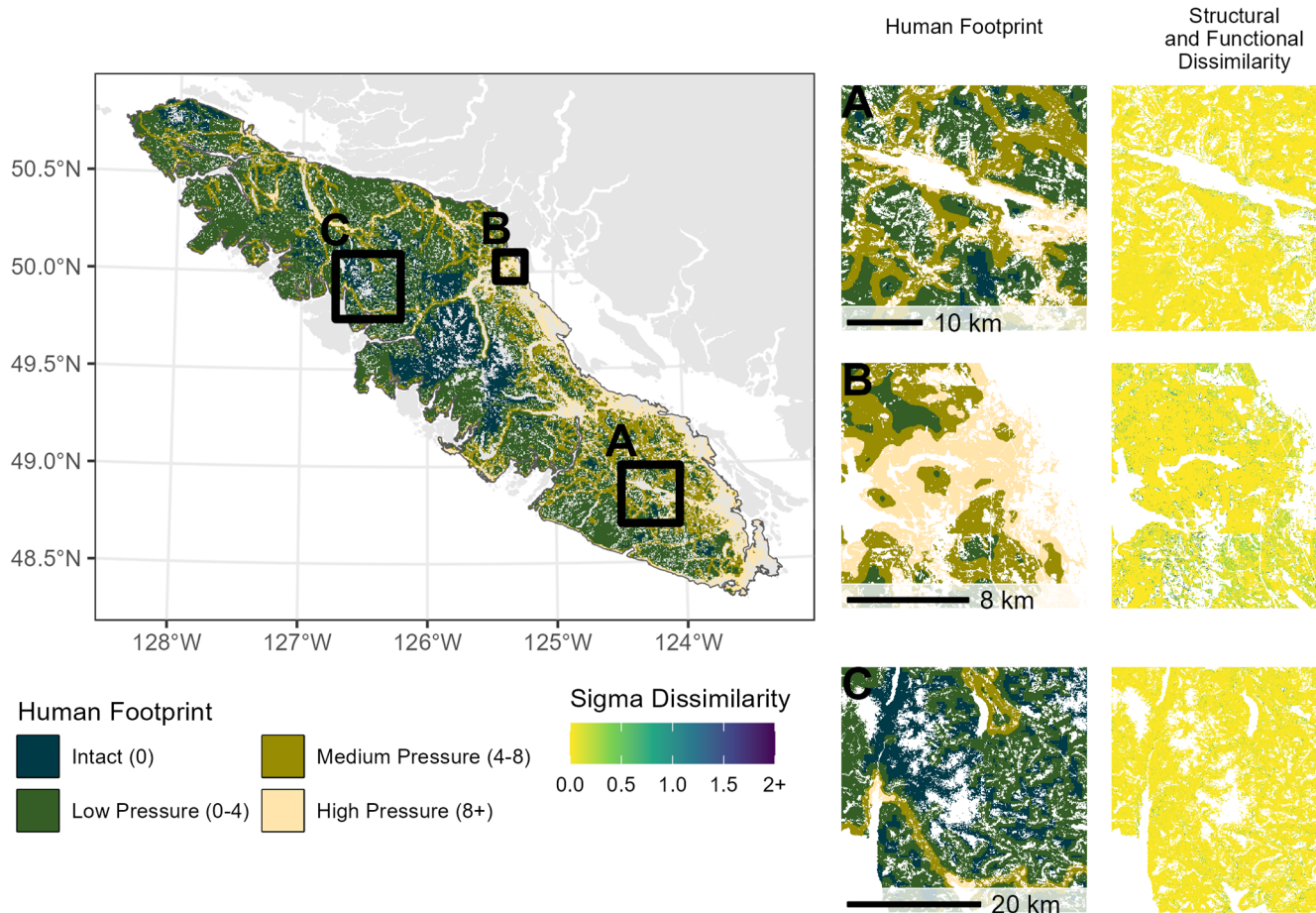


Figure 4: Regional details of the human footprint and sigma dissimilarity across the sites on Vancouver Island. Subset A shows Cowichan Lake, a heavily harvested region. Subset B shows Elk Falls Provincial Park, just outside Campbell River, a region with high population density. Subset C shows a region with generally low anthropogenic pressure.

We used ANOVAs and post-hoc Tukey HSD tests to assess the influence of the cumulative human footprint on ecological dissimilarity (Figure 5). Results indicate that structural (ANOVA; $p = 0.014$) and structural + functional (ANOVA; $p = 0.006$) dissimilarity was significantly different under varying anthropogenic pressures. The functional dissimilarity metric did not significantly vary with anthropogenic pressures. The Tukey HSD test revealed that high levels of anthropogenic pressures significantly influence dissimilarity to the structural (ANOVA; $p < 0.01$) and structural + functional (ANOVA; $p < 0.05$) reference state. Medium and low levels of anthropogenic pressures did not significantly influence any dissimilarity metrics.

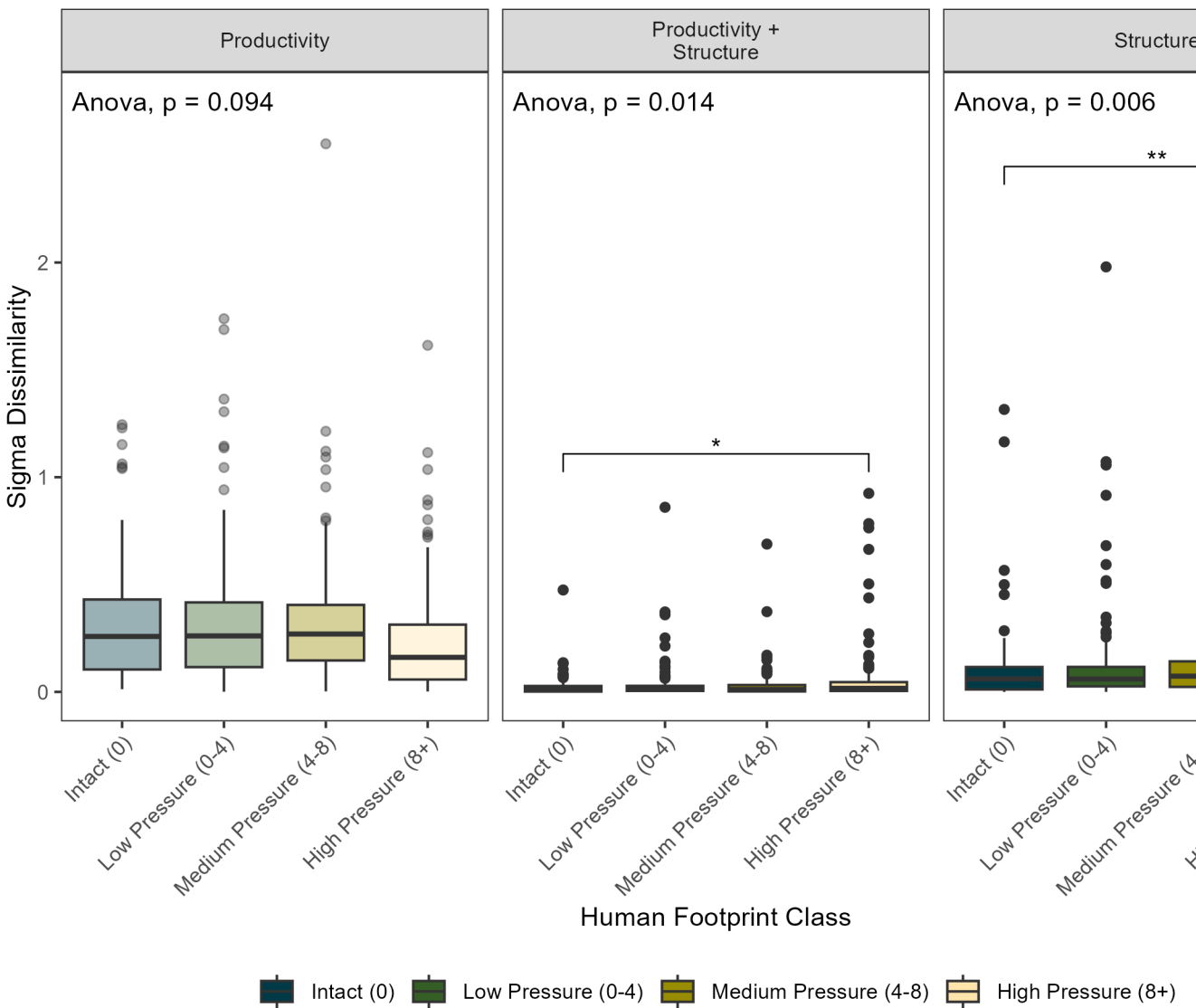


Figure 5: Boxplots of sigma similarity to the reference state in Strathcona Provincial Park by cumulative human footprint category. ANOVA p-values corrected using the Holm-Bonferroni method. * indicates a Tukey HSD p-value < 0.05. ** indicates a Tukey HSD p-value < 0.01.

Further we assessed the impact of individual pressures on ecological dissimilarity to the reference state (Figure 6). We found that functional dissimilarity was not significantly influenced by any anthropogenic pressures, and that roads did not influence any type of ecological dissimilarity (ANOVAs; all $p > 0.05$). Population density, forestry and harvesting, and built environments did significantly increase both structural and structural + functional dissimilarity (ANOVAs; all $p < 0.01$). Only the highest levels of pressures for each anthropogenic pressure category significantly influenced ecological dissimilarity (ANOVAs; all $p < 0.01$).

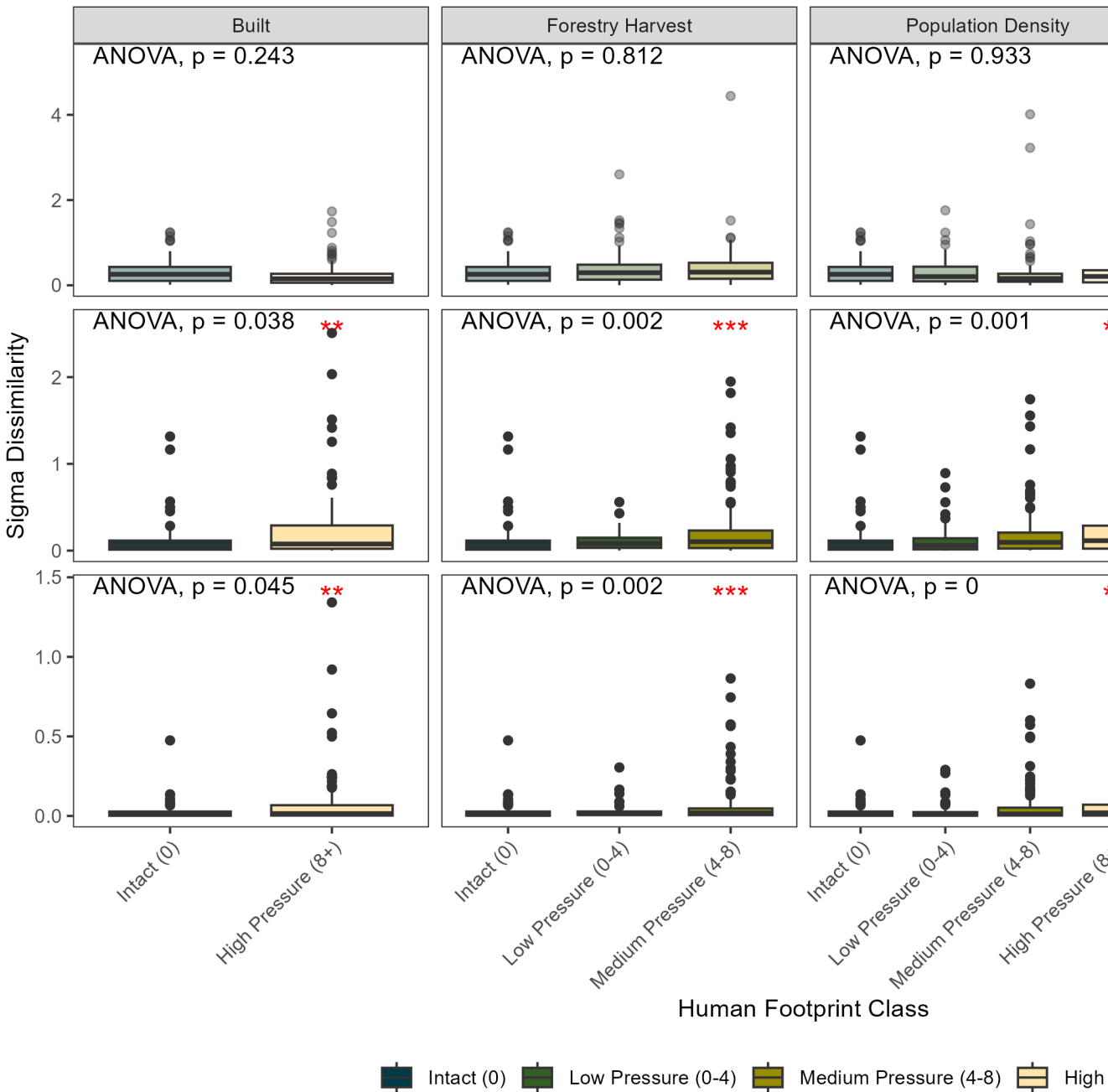


Figure 6: Boxplots of sigma similarity to the reference state in Strathcona Provincial Park by individual anthropogenic pressures. ANOVA p-values corrected using the Holm-Bonferroni method. ** indicates a Tukey HSD p-value < 0.01 . *** indicates a Tukey HSD p-value < 0.001 .

Discussion

Here, we propose a novel approach to assess ecological integrity across forested ecosystems. Our method incorporates an expanded coarsened exact matching technique (Iacus et al., 2012) and a multidimensional dissimilarity metric (Mahony et al., 2017). This method integrates a robust method for generating suitable refer-

ence states through the use of a large, long-term protected area, and excluding any pressures and disturbances, and estimates ecological integrity as dissimilarity to the reference state by using the sigma dissimilarity metric, which accounts for covariations in the data and varying dimensionality in input datasets. The methodology is demonstrated on the forested areas of Vancouver Island, which are environmentally similar to the reference state, Strathcona Park. Furthermore, the influence of anthropogenic pressure on ecological integrity is assessed. It was found that high levels of anthropogenic pressure increase structural and structural + functional dissimilarity, thus showing a reduction in ecological integrity (Figure 5; Figure 6). However, functional dissimilarity was never influenced by anthropogenic pressures.

Our structural dissimilarity metric is similar to other metrics of forest condition, such as the forest structural condition index (Hansen et al., 2019), however, it is not reliant on expert-set thresholds. This potentially allows our metric to be transferable to new ecosystems and environments, even allowing for the assessment of dissimilarity for other ecosystems or a species' core ranges by changing the reference state. This could be important for conservation efforts of rare and threatened species. Further, we found that high cumulative anthropogenic pressures increases structural dissimilarity (Figure 5), and that high individual pressures, except roads, also increase structural dissimilarity (Figure 6). Prior research has generally focused on tropical forests, where Bourgoin et al. (2024) found that anthropogenic forest degradation influenced aboveground biomass and canopy height, however, they focus on edge effects, fire, and selective logging, rather than cumulative and individual anthropogenic pressures. Li et al. (2023) also found a global impact of anthropogenic pressures on forest structural density; however, they do not explore which facets of anthropogenic pressure are the strongest driver of forest degradation. Hansen et al. (2020) integrate forest structure and anthropogenic pressure into the forest structural integrity index to identify forest stands of high ecological value (high structural quality; low anthropogenic footprint). We further this body of research by assessing individual pressures on a multivariate metric of structural similarity to a high-quality reference state (Figure 6). While we assess impacts of pressures on structural dissimilarity, integrating them together, similar to Hansen et al. (2020), could help with protected area prioritization efforts outside of moist tropical forests.

We also assess functional dissimilarity to high-integrity forests. We found that functional dissimilarity more strongly varies than structural dissimilarity (Figure 4). However, we did not find any significant influence of cumulative or individual anthropogenic pressures on our forest functioning metrics (Figure 5; Figure 6). This may in part be due to the DHIs reliance on vegetation indices or productivity estimates, in our case NDVI. Vegetation indices have been shown to saturate at high levels of canopy cover and leaf area index (Huete et al., 2002; Huete et al., 1997), which are common in our study area. Recent research has shown that seasonality, here represented as the Variation DHI, drives functional diversity in avian assemblages, however, these results also strongly varied by region (Keyser et al., 2024). It is possible that examining anthropogenic pressure impacts in regions with more variation in canopy cover and stronger seasonality may lead to differing results, as Vancouver Island has a moderate climate, and is primarily dominated by conifer species Section .

We identified high-integrity forest reference states across a large region using a data-driven approach. Often, it is common for suitable reference states to be unavailable due to a lack of data on regions of high ecological integrity, especially across large regions (McNellie et al., 2020). We attempt to circumvent this by using a large, long-established protected area (Strathcona Provincial Park; Figure 1), and a matching technique that preserves environmental similarity between reference states and their counterparts. The long-established, large protected area ensures that little anthropogenic pressures or modification have been made to the landscape, while also

390 guaranteeing that the reference state is attainable for a given topography and cli-
 391 mate (Corlett, 2016; Hobbs et al., 2014) due to contemporary nature of the reference
 392 state. Our matching technique (coarsened exact matching, combined with a nearest
 393 neighbour approach when no exact match is available) allows us to generate refer-
 394 ence states in a near wall-to-wall fashion, which ensures environmental consistency
 395 between reference state and compared pixels.

396 Our techniques move beyond traditional impact evaluation techniques (Ferraro,
 397 2009) commonly used in protected area effectiveness assessments by generating
 398 spatially explicit maps of ecological dissimilarity, and generating a multivariate,
 399 rather than univariate, assessment of similarity to high ecological integrity forests.
 400 While our methods use a data-driven approach to derive reference states using a
 401 high-quality protected area, the method is inherently reference state agnostic. Dis-
 402 similarity metrics could be generated for a specific ecosystem, species, or community
 403 at landscape scales, identifying areas with similar structural and functional condi-
 404 tions. This could be especially relevant for species with known habitat requirements,
 405 such as the marbled murrelet (*Brachyramphus marmoratus*) needing tall, complex
 406 forests as nesting habitat (Cosgrove et al., 2024)

407 Assessing individual pressure influences on the environment is also relevant to ques-
 408 tions of how cumulative anthropogenic pressure maps are calculated. There is an
 409 ongoing debate surrounding anthropogenic pressure mapping methods, as there is
 410 little information on mechanistic interactions between pressures (Arias-Patino et
 411 al., 2024). We assess individual pressures on ecological dissimilarity in forests across
 412 Vancouver Island, Canada, an advancement upon the current standard of using a
 413 single value of cumulative anthropogenic pressure (Bourgoin et al., 2024; Li et al.,
 414 2023). Similar methods could be used to examine mechanistic pressure interactions
 415 across large scales by examining combinations of pressures rather than individual or
 416 overall impacts.

417 Conclusion

418 Identifying the location of high-integrity forests is integral to conservation efforts,
 419 especially when considering protected area management (Hansen et al., 2021; Pillay
 420 et al., 2024a). Until recently, area based conservation has dominated management
 421 strategies, which does not ensure that high-integrity ecosystems, typically hav-
 422 ing high biodiversity and ecosystem services present, are protected (Ferrier et al.,
 423 2024; Pillay et al., 2024a). Recent efforts to identify high-integrity forests have been
 424 primarily focused on moist tropical forests (Hansen et al., 2019), which contain
 425 large numbers of threatened species reliant on intact forest structures (Pillay et al.,
 426 2024b). Due to their focus on moist tropical forests, their methodology cannot eas-
 427 ily be transferred to other forested ecosystems, particularly due to their focus on
 428 tall, complex trees (Hansen et al., 2019) without considering local environmental
 429 conditions. Here, we use matching techniques to circumvent this, and use sigma dis-
 430 similarity to consider additional structural and functional information, allowing us
 431 to identify high-integrity forests without relying on expert defined thresholds which
 432 may not be suitable or available in all biomes. This advance can be used to conser-
 433 vation planning strategies, as we work towards the 30x30 goal outlined in the GBF
 434 (Convention on Biological Diversity, 2023).

435 Acknowledgements

436 This research was funded by NSERC support of Coops (RGPIN-2024-04402).
 437 Remote sensing data products used in this research are free and open and avail-
 438 able for download at https://ca.nfis.org/maps_eng.html. The authors thank
 439 Dr. Michael A. Wulder and Dr. Joanne C. White for development and early access
 440 to these National Terrestrial Ecosystem Mapping System (NTEMS) products. They
 441 thank Dr. Elena Razenkova for early access to the Landsat-derived Dynamic Habi-

⁴⁴² tat Indices. ERM would like to thank the members of the IRSS for many helpful
⁴⁴³ conversations throughout the preparation of this manuscript.

⁴⁴⁴ **Ethics**

⁴⁴⁵ The authors declare no conflicts of interest.

446 **References**

- 447 Abrams, M., Crippen, R., Fujisada, H., 2020. ASTER Global Digital Elevation
 448 Model (GDEM) and ASTER Global Water Body Dataset (ASTWBD). *Remote*
 449 *Sensing* 12, 1156. <https://doi.org/10.3390/rs12071156>
- 450 Ali, A., 2019. Forest stand structure and functioning: Current knowledge and fu-
 451 ture challenges. *Ecological Indicators* 98, 665–677. <https://doi.org/10.1016/j.ecolind.2018.11.017>
- 452 Andrew, M.E., Bolton, D.K., Rickbeil, G.J.M., Coops, N.C., 2024. Facets of func-
 453 tional diversity support niche-based explanations for Australian biodiversity
 454 gradients. *Journal of Biogeography* 51, 467–482. <https://doi.org/10.1111/jbi.14770>
- 455 Andrew, M.E., Wulder, M.A., Coops, N.C., Baillargeon, G., 2012. Beta-diversity
 456 gradients of butterflies along productivity axes. *Global Ecology and Biogeogra-
 457 phy* 21, 352–364. <https://doi.org/10.1111/j.1466-8238.2011.00676.x>
- 458 Arcese, P., Sinclair, A.R.E., 1997. The role of protected areas as ecological baselines.
 459 *The Journal of Wildlife Management* 61, 587–602. <https://doi.org/10.2307/3802167>
- 460 Arias-Patino, M., Johnson, C.J., Schuster, R., Wheate, R.D., Venter, O., 2024.
 461 Accuracy, uncertainty, and biases in cumulative pressure mapping. *Ecological
 462 Indicators* 166, 112407. <https://doi.org/10.1016/j.ecolind.2024.112407>
- 463 Bergen, K.M., Goetz, S.J., Dubayah, R.O., Henebry, G.M., Hunsaker, C.T., Imhoff,
 464 M.L., Nelson, R.F., Parker, G.G., Radeloff, V.C., 2009. Remote sensing of veg-
 465 etation 3-d structure for biodiversity and habitat: Review and implications
 466 for lidar and radar spaceborne missions. *Journal of Geophysical Research-
 467 Biogeosciences* 114, G00E06. <https://doi.org/10.1029/2008JG000883>
- 468 Berry, S., Mackey, B., Brown, T., 2007. Potential applications of remotely sensed
 469 vegetation greenness to habitat analysis and the conservation of dispersive fauna.
 470 *Pacific Conservation Biology* 13, 120–127. <https://doi.org/10.1071/PC070120>
- 471 Bourgoin, C., Ceccherini, G., Girardello, M., Vancutsem, C., Avitabile, V., Beck,
 472 P.S.A., Beuchle, R., Blanc, L., Duveiller, G., Migliavacca, M., Vieilledent, G.,
 473 Cescatti, A., Achard, F., 2024. Human degradation of tropical moist forests is
 474 greater than previously estimated. *Nature* 631, 570–576. <https://doi.org/10.1038/s41586-024-07629-0>
- 475 Burns, R.M., 1990. Silvics of North America. U.S. Department of Agriculture, For-
 476 est Service.
- 477 Cardinale, B.J., Duffy, J.E., Gonzalez, A., Hooper, D.U., Perrings, C., Venail,
 478 P., Narwani, A., Mace, G.M., Tilman, D., Wardle, D.A., Kinzig, A.P., Daily,
 479 G.C., Loreau, M., Grace, J.B., Larigauderie, A., Srivastava, D.S., Naeem,
 480 S., 2012. Biodiversity loss and its impact on humanity. *Nature* 486, 59–67.
 481 <https://doi.org/10.1038/nature11148>
- 482 Convention on Biological Diversity, 2023. Report of the conference of the parties to
 483 the Convention on Biological Diversity on the second part of its fifteenth meeting
 484 (No. CBD/COP/15/17).
- 485 Coops, N.C., Bolton, D.K., Hobi, M.L., Radeloff, V.C., 2019. Untangling multiple
 486 species richness hypothesis globally using remote sensing habitat indices. *Ecolog-
 487 ical Indicators* 107. <https://doi.org/10.1016/j.ecolind.2019.105567>
- 488 Coops, N.C., Waring, R.H., Wulder, M.A., Pidgeon, A.M., Radeloff, V.C., 2009a.
 489 Bird diversity: A predictable function of satellite-derived estimates of seasonal
 490 variation in canopy light absorbance across the United States. *Journal of Bio-
 491 geography* 36, 905–918. <https://doi.org/10.1111/j.1365-2699.2008.02053.x>
- 492 Coops, N.C., Wulder, M.A., Iwanicka, D., 2009b. Demonstration of a satellite-based
 493 index to monitor habitat at continental-scales. *Ecological Informatics* 9, 948–958.
 494 <https://doi.org/10.1016/j.ecolind.2008.11.003>

- 499 Corlett, R.T., 2016. Restoration, reintroduction, and rewilding in a changing world.
 500 Trends in Ecology & Evolution 31, 453–462. <https://doi.org/10.1016/j.tree.2016.02.017>
- 502 Cosgrove, C.F., Coops, N.C., Waterhouse, F.L., Goodbody, T.R.H., 2024. Modeling
 503 marbled murrelet nesting habitat: A quantitative approach using airborne laser
 504 scanning data in british columbia, canada. Avian Conservation and Ecology 19.
 505 <https://doi.org/10.5751/ACE-02585-190105>
- 506 Daniels, L.D., Gray, R.W., 2006. Disturbance regimes in coastal British Columbia.
 507 Journal of Ecosystems and Management 7. <https://doi.org/10.22230/jem.2006v7n2a542>
- 509 Duncanson, L., Liang, M., Leitold, V., Armston, J., Krishna Moorthy, S.M., Dubayah,
 510 R., Costedoat, S., Enquist, B.J., Fatoyinbo, L., Goetz, S.J., Gonzalez-Roglich,
 511 M., Merow, C., Roehrdanz, P.R., Tabor, K., Zvoleff, A., 2023. The effectiveness
 512 of global protected areas for climate change mitigation. Nature Communications
 513 14, 2908. <https://doi.org/10.1038/s41467-023-38073-9>
- 514 Ferraro, P.J., 2009. Counterfactual thinking and impact evaluation in environmental
 515 policy. New Directions for Evaluation 2009, 75–84. <https://doi.org/10.1002/ev.297>
- 517 Ferrier, S., Ware, C., Austin, J.M., Grantham, H.S., Harwood, T.D., Watson,
 518 J.E.M., 2024. Ecosystem extent is a necessary but not sufficient indicator
 519 of the state of global forest biodiversity. Conservation Letters 17, e13045.
 520 <https://doi.org/10.1111/conl.13045>
- 521 Gao, T., Hedblom, M., Emilsson, T., Nielsen, A.B., 2014. The role of forest stand
 522 structure as biodiversity indicator. Forest Ecology and Management 330, 82–93.
 523 <https://doi.org/10.1016/j.foreco.2014.07.007>
- 524 Geldmann, J., Manica, A., Burgess, N.D., Coad, L., Balmford, A., 2019. A global-
 525 level assessment of the effectiveness of protected areas at resisting anthropogenic
 526 pressures. Proceedings of the National Academy of Sciences 116, 23209–23215.
 527 <https://doi.org/10.1073/pnas.1908221116>
- 528 Goodbody, T.R.H., Coops, N.C., Queinnec, M., White, J.C., Tompalski, P., Hu-
 529 dak, A.T., Auty, D., Valbuena, R., LeBoeuf, A., Sinclair, I., McCartney, G.,
 530 Prieur, J.-F., Woods, M.E., 2023. sgsR: A structurally guided sampling toolbox
 531 for LiDAR-based forest inventories. Forestry: An International Journal of Forest
 532 Research 96, 411–424. <https://doi.org/10.1093/forestry/cpac055>
- 533 Gorelick, N., Hancher, M., Dixon, M., Ilyushchenko, S., Thau, D., Moore, R., 2017.
 534 Google Earth Engine: Planetary-scale geospatial analysis for everyone. Remote
 535 Sensing of Environment, Big Remotely Sensed Data: tools, applications and
 536 experiences 202, 18–27. <https://doi.org/10.1016/j.rse.2017.06.031>
- 537 Grantham, H.S., Duncan, A., Evans, T.D., Jones, K.R., Beyer, H.L., Schuster,
 538 R., Walston, J., Ray, J.C., Robinson, J.G., Callow, M., Clements, T., Costa,
 539 H.M., DeGennmis, A., Elsen, P.R., Ervin, J., Franco, P., Goldman, E., Goetz,
 540 S., Hansen, A., Hofsvang, E., Jantz, P., Jupiter, S., Kang, A., Langhammer, P.,
 541 Laurance, W.F., Lieberman, S., Linkie, M., Malhi, Y., Maxwell, S., Mendez,
 542 M., Mittermeier, R., Murray, N.J., Possingham, H., Radachowsky, J., Saatchi,
 543 S., Samper, C., Silverman, J., Shapiro, A., Strassburg, B., Stevens, T., Stokes,
 544 E., Taylor, R., Tear, T., Tizard, R., Venter, O., Visconti, P., Wang, S., Wat-
 545 son, J.E.M., 2020. Anthropogenic modification of forests means only 40. Nature
 546 Communications 11, 5978. <https://doi.org/10.1038/s41467-020-19493-3>
- 547 Guo, X., Coops, N.C., Tompalski, P., Nielsen, S.E., Bater, C.W., John Stadt, J.,
 548 2017. Regional mapping of vegetation structure for biodiversity monitoring us-
 549 ing airborne lidar data. Ecological Informatics 38, 50–61. <https://doi.org/10.1016/j.ecoinf.2017.01.005>
- 550 Hansen, A., Barnett, K., Jantz, P., Phillips, L., Goetz, S.J., Hansen, M., Venter,
 551 O., Watson, J.E.M., Burns, P., Atkinson, S., Rodríguez-Buriticá, S., Ervin, J.,
 552 Virnig, A., Supples, C., De Camargo, R., 2019. Global humid tropics forest
 553

- 554 structural condition and forest structural integrity maps. *Scientific Data* 6, 232.
 555 <https://doi.org/10.1038/s41597-019-0214-3>
- 556 Hansen, A.J., Burns, P., Ervin, J., Goetz, S.J., Hansen, M., Venter, O., Watson,
 557 J.E.M., Jantz, P.A., Virnig, A.L.S., Barnett, K., Pillay, R., Atkinson, S., Sup-
 558 ples, C., Rodríguez-Buriticá, S., Armenteras, D., 2020. A policy-driven frame-
 559 work for conserving the best of Earth's remaining moist tropical forests. *Nature
 560 Ecology & Evolution* 4, 1377–1384. <https://doi.org/10.1038/s41559-020-1274-7>
- 561 Hansen, A.J., Noble, B.P., Veneros, J., East, A., Goetz, S.J., Supples, C., Watson,
 562 J.E.M., Jantz, P.A., Pillay, R., Jetz, W., Ferrier, S., Grantham, H.S., Evans,
 563 T.D., Ervin, J., Venter, O., Virnig, A.L.S., 2021. Toward monitoring forest
 564 ecosystem integrity within the post-2020 Global Biodiversity Framework. *Conser-
 565 vation Letters* 14, e12822. <https://doi.org/10.1111/conl.12822>
- 566 Hermosilla, T., Wulder, M.A., White, J.C., Coops, N.C., Hobart, G.W., 2018.
 567 Disturbance-informed annual land cover classification maps of canada's forested
 568 ecosystems for a 29-year landsat time series. *Canadian Journal of Remote Sens-
 569 ing* 44, 6787. <https://doi.org/10.1080/07038992.2018.1437719>
- 570 Hermosilla, T., Wulder, M.A., White, J.C., Coops, N.C., Hobart, G.W., 2015. An
 571 integrated landsat time series protocol for change detection and generation of
 572 annual gap-free surface reflectance composites. *Remote Sensing of Environment*
 573 158, 220234. <https://doi.org/10.1016/j.rse.2014.11.005>
- 574 Hermosilla, T., Wulder, M.A., White, J.C., Coops, N.C., Hobart, G.W., Camp-
 575 bell, L.B., 2016. Mass data processing of time series landsat imagery: Pixels to
 576 data products for forest monitoring. *International Journal of Digital Earth* 9,
 577 10351054. <https://doi.org/10.1080/17538947.2016.1187673>
- 578 Hernangómez, D., 2023. Using the tidyverse with terra objects: The tidyterra pack-
 579 age. *Journal of Open Source Software* 8, 5751. <https://doi.org/10.21105/joss.05751>
- 580 Hijmans, R.J., 2024. *Terra: Spatial data analysis*.
- 581 Hirsh-Pearson, K., Johnson, C.J., Schuster, R., Wheate, R.D., Venter, O., 2022.
 582 Canada's human footprint reveals large intact areas juxtaposed against areas
 583 under immense anthropogenic pressure. *FACETS* 7, 398–419. <https://doi.org/10.1139/facets-2021-0063>
- 584 Hirsh-Pearson, K., Johnson, C., Schuster, R., Wheate, R., Venter, O., n.d. The
 585 Canadian Human Footprint. <https://doi.org/10.5683/SP2/EVKAVL>
- 586 Hobbs, R.J., Higgs, E., Hall, C.M., Bridgewater, P., Chapin III, F.S., Ellis, E.C.,
 587 Ewel, J.J., Hallett, L.M., Harris, J., Hulvey, K.B., Jackson, S.T., Kennedy, P.L.,
 588 Kueffer, C., Lach, L., Lantz, T.C., Lugo, A.E., Mascaro, J., Murphy, S.D., Nel-
 589 son, C.R., Perring, M.P., Richardson, D.M., Seastedt, T.R., Standish, R.J., Star-
 590 zomski, B.M., Suding, K.N., Tognetti, P.M., Yakob, L., Yung, L., 2014. Manag-
 591 ing the whole landscape: historical, hybrid, and novel ecosystems. *Frontiers in
 592 Ecology and the Environment* 12, 557–564. <https://doi.org/10.1890/130300>
- 593 Holm, S., 1979. *A simple sequentially rejective multiple test procedure*. *Scandina-
 594 vian Journal of Statistics* 6, 65–70.
- 595 Huete, A., Didan, K., Miura, T., Rodriguez, E.P., Gao, X., Ferreira, L.G., 2002.
 596 Overview of the radiometric and biophysical performance of the MODIS vegeta-
 597 tion indices. *Remote Sensing of Environment* 83, 195–213. [https://doi.org/10.1016/S0034-4257\(02\)00096-2](https://doi.org/10.1016/S0034-4257(02)00096-2)
- 598 Huete, A.R., Liu, H., Leeuwen, W.J.D. van, 1997. IGARSS'97. 1997 IEEE in-
 599 ternational geoscience and remote sensing symposium proceedings. *Remote
 600 sensing - a scientific vision for sustainable development.* pp. 1966–1968 vol.4.
 601 <https://doi.org/10.1109/IGARSS.1997.609169>
- 602 Iacus, S.M., King, G., Porro, G., 2012. Causal Inference without Balance Check-
 603 ing: Coarsened Exact Matching. *Political Analysis* 20, 1–24. <https://doi.org/10.1093/pan/mpr013>

- 609 Joppa, L.N., Pfaff, A., 2009. High and Far: Biases in the Location of Protected Ar-
 610 eas. PLOS ONE 4, e8273. <https://doi.org/10.1371/journal.pone.0008273>
- 611 Kassambara, A., 2023. Rstatix: Pipe-friendly framework for basic statistical tests.
- 612 Keyser, S.R., Pauli, J.N., Fink, D., Radloff, V.C., Pigot, A.L., Zuckerberg, B.,
 613 2024. Seasonality Structures Avian Functional Diversity and Niche Packing
 614 Across North America. Ecology Letters 27, e14521. <https://doi.org/10.1111/ele.14521>
- 615 Li, W., Guo, W.-Y., Pasgaard, M., Niu, Z., Wang, L., Chen, F., Qin, Y., Svenning,
 616 J.-C., 2023. Human fingerprint on structural density of forests globally. Nature
 617 Sustainability 6, 368–379. <https://doi.org/10.1038/s41893-022-01020-5>
- 618 MacArthur, R., MacArthur, J., 1961. On bird species-diversity. Ecology 42, 594– &.
 619 <https://doi.org/10.2307/1932254>
- 620 Mahalanobis, P.C., 1936. On the generalized distance in statistics. Proceedings of
 621 the National Institute of Sciences (Calcutta) 2, 4955.
- 622 Mahony, C.R., Cannon, A.J., Wang, T., Aitken, S.N., 2017. A closer look at novel
 623 climates: new methods and insights at continental to landscape scales. Global
 624 Change Biology 23, 3934–3955. <https://doi.org/10.1111/gcb.13645>
- 625 Marín, A.I., Abdul Malak, D., Bastrup-Birk, A., Chirici, G., Barbuti, A., Kleeschulte,
 626 S., 2021. Mapping forest condition in europe: Methodological developments in
 627 support to forest biodiversity assessments. Ecological Indicators 128, 107839.
 628 <https://doi.org/10.1016/j.ecolind.2021.107839>
- 629 Matasci, G., Hermosilla, T., Wulder, M.A., White, J.C., Coops, N.C., Hobart, G.W.,
 630 Bolton, D.K., Tompalski, P., Bater, C.W., 2018a. Three decades of forest struc-
 631 tural dynamics over canada’s forested ecosystems using landsat time-series and
 632 lidar plots. Remote Sensing of Environment 216, 697714. <https://doi.org/10.1016/j.rse.2018.07.024>
- 633 Matasci, G., Hermosilla, T., Wulder, M.A., White, J.C., Coops, N.C., Hobart, G.W.,
 634 Zald, H.S.J., 2018b. Large-area mapping of Canadian boreal forest cover, height,
 635 biomass and other structural attributes using Landsat composites and lidar
 636 plots. Remote Sensing of Environment 209, 90–106. <https://doi.org/10.1016/j.rse.2017.12.020>
- 637 McNellie, M.J., Oliver, I., Dorrough, J., Ferrier, S., Newell, G., Gibbons, P., 2020.
 638 Reference state and benchmark concepts for better biodiversity conservation
 639 in contemporary ecosystems. Global Change Biology 26, 6702–6714. <https://doi.org/10.1111/gcb.15383>
- 640 Michaud, J.-S., Coops, N.C., Andrew, M.E., Wulder, M.A., Brown, G.S., Rickbeil,
 641 G.J.M., 2014. Estimating moose (*alces alces*) occurrence and abundance from
 642 remotely derived environmental indicators. Remote Sensing of Environment 152,
 643 190–201. <https://doi.org/10.1016/j.rse.2014.06.005>
- 644 Ministry of Water, Land and Resource Stewardship (WLRS), 2023. Current condi-
 645 tion report for old growth forest on vancouver island - 2019 analysis.
- 646 Muise, E.R., Andrew, M.E., Coops, N.C., Hermosilla, T., Burton, A.C., Ban, S.S.,
 647 2024. Disentangling linkages between satellite-derived indicators of forest struc-
 648 ture and productivity for ecosystem monitoring. Scientific Reports 14, 13717.
 649 <https://doi.org/10.1038/s41598-024-64615-2>
- 650 Muise, E.R., Coops, N.C., Hermosilla, T., Ban, S.S., 2022. Assessing representation
 651 of remote sensing derived forest structure and land cover across a network of
 652 protected areas. Ecological Applications 32, e2603. <https://doi.org/10.1002/eap.2603>
- 653 Myers, N., 1988. Threatened biotas: "Hot spots" in tropical forests. Environmental-
 654 ist 8, 187–208. <https://doi.org/10.1007/BF02240252>
- 655 Naidoo, R., Ricketts, T.H., 2006. Mapping the economic costs and benefits of con-
 656 servation. PLoS Biology 4, 2153–2164. <https://doi.org/10.1371/journal.pbio.0040360>

- 663 Nicholson, E., Watermeyer, K.E., Rowland, J.A., Sato, C.F., Stevenson, S.L.,
 664 Andrade, A., Brooks, T.M., Burgess, N.D., Cheng, S.-T., Grantham, H.S.,
 665 Hill, S.L., Keith, D.A., Maron, M., Metzke, D., Murray, N.J., Nelson, C.R.,
 666 Obura, D., Plumptre, A., Skowno, A.L., Watson, J.E.M., 2021. Scientific foun-
 667 dations for an ecosystem goal, milestones and indicators for the post-2020
 668 global biodiversity framework. *Nature Ecology & Evolution* 5, 1338–1349.
 669 <https://doi.org/10.1038/s41559-021-01538-5>
- 670 Nielsen, S.E., Bayne, E.M., Schieck, J., Herbers, J., Boutin, S., 2007. A new method
 671 to estimate species and biodiversity intactness using empirically derived reference
 672 conditions. *Biological Conservation* 137, 403–414. <https://doi.org/10.1016/j.biocon.2007.02.024>
- 673 Park Act, 1996. RSBC 1996, c 344.
- 674 Pebesma, E., 2018. Simple Features for R: Standardized Support for Spatial Vector
 675 Data. *The R Journal* 10, 439–446. <https://doi.org/10.32614/RJ-2018-009>
- 676 Pebesma, E., Bivand, R., 2023. Spatial Data Science: With applications in R. Chap-
 677 man and Hall/CRC. <https://doi.org/10.1201/9780429459016>
- 678 Pereira, H.M., Ferrier, S., Walters, M., Geller, G.N., Jongman, R.H.G., Scholes,
 679 R.J., Bruford, M.W., Brummitt, N., Butchart, S.H.M., Cardoso, A.C., Coops,
 680 N.C., Dulloo, E., Faith, D.P., Freyhof, J., Gregory, R.D., Heip, C., Hoft, R.,
 681 Hurtt, G., Jetz, W., Karp, D.S., McGeoch, M.A., Obura, D., Onoda, Y., Pet-
 682 torelli, N., Reyers, B., Sayre, R., Scharlemann, J.P.W., Stuart, S.N., Turak, E.,
 683 Walpole, M., Wegmann, M., 2013. Essential Biodiversity Variables. *Science* 339,
 684 277–278. <https://doi.org/10.1126/science.1229931>
- 685 Pettorelli, N., Schulte to Bühne, H., Tulloch, A., Dubois, G., Macinnis-Ng, C.,
 686 Queirós, A.M., Keith, D.A., Wegmann, M., Schrodt, F., Stellmes, M., Son-
 687 nvenschein, R., Geller, G.N., Roy, S., Somers, B., Murray, N., Bland, L., Gei-
 688 jzendorffer, I., Kerr, J.T., Broszeit, S., Leitão, P.J., Duncan, C., El Serafy,
 689 G., He, K.S., Blanchard, J.L., Lucas, R., Mairotta, P., Webb, T.J., Nicholson,
 690 E., 2018. Satellite remote sensing of ecosystem functions: opportunities, chal-
 691 lenges and way forward. *Remote Sensing in Ecology and Conservation* 4, 71–93.
 692 <https://doi.org/10.1002/rse2.59>
- 693 Pettorelli, N., Vik, J.O., Mysterud, A., Gaillard, J.-M., Tucker, C.J., Stenseth,
 694 N.Chr., 2005. Using the satellite-derived NDVI to assess ecological responses to
 695 environmental change. *Trends in Ecology & Evolution* 20, 503–510. <https://doi.org/10.1016/j.tree.2005.05.011>
- 696 Pillay, R., Watson, J.E.M., Goetz, S.J., Hansen, A.J., Jantz, P.A., Ramírez-Delgado,
 697 J.P., Grantham, H.S., Ferrier, S., Venter, O., 2024a. The Kunming-Montreal
 698 Global Biodiversity Framework needs headline indicators that can actually mon-
 699 itor forest integrity. *Environmental Research: Ecology* 3, 043001. <https://doi.org/10.1088/2752-664X/ad7961>
- 700 Pillay, R., Watson, J.E.M., Hansen, A.J., Burns, P., Virnig, A.L.S., Supples, C.,
 701 Armenteras, D., González-del-Pliego, P., Aragón-Osejo, J., A. Jantz, P., Ervin,
 702 J., Goetz, S.J., Venter, O., 2024b. Global rarity of high-integrity tropical rain-
 703 forests for threatened and declining terrestrial vertebrates. *Proceedings of the
 704 National Academy of Sciences* 121, e2413325121. <https://doi.org/10.1073/pnas.2413325121>
- 705 Pimm, S.L., Raven, P., 2000. Extinction by numbers. *Nature* 403, 843–845. <https://doi.org/10.1038/35002708>
- 706 Pojar, J., Klinka, K., Meidinger, D.V., 1987. Biogeoclimatic ecosystem classi-
 707 fication in British Columbia. *Forest Ecology and Management* 22, 119–154.
 708 [https://doi.org/10.1016/0378-1127\(87\)90100-9](https://doi.org/10.1016/0378-1127(87)90100-9)
- 709 Potapov, P., Li, X., Hernandez-Serna, A., Tyukavina, A., Hansen, M.C., Kom-
 710 mareddy, A., Pickens, A., Turubanova, S., Tang, H., Silva, C.E., Armston, J.,
 711 Dubayah, R., Blair, J.B., Hofton, M., 2021. Mapping global forest canopy height
 712

- 717 through integration of GEDI and Landsat data. *Remote Sensing of Environment*
 718 253, 112165. <https://doi.org/10.1016/j.rse.2020.112165>
- 719 Queinnec, M., White, J.C., Coops, N.C., 2021. Comparing airborne and spaceborne
 720 photon-counting LiDAR canopy structural estimates across different boreal for-
 721 est types. *Remote Sensing of Environment* 262, 112510. <https://doi.org/10.1016/j.rse.2021.112510>
- 723 R Core Team, 2024. *R: A language and environment for statistical computing*. R
 724 Foundation for Statistical Computing, Vienna, Austria.
- 725 Radeloff, V.C., Dubinin, M., Coops, N.C., Allen, A.M., Brooks, T.M., Clayton,
 726 M.K., Costa, G.C., Graham, C.H., Helmers, D.P., Ives, A.R., Kolesov, D., Pid-
 727 geon, A.M., Rapacciulo, G., Razenkova, E., Suttidate, N., Young, B.E., Zhu, L.,
 728 Hobi, M.L., 2019. The Dynamic Habitat Indices (DHIs) from MODIS and global
 729 biodiversity. *Remote Sensing of Environment* 222, 204–214. <https://doi.org/10.1016/j.rse.2018.12.009>
- 731 Radeloff, V.C., Roy, D.P., Wulder, M.A., Anderson, M., Cook, B., Crawford, C.J.,
 732 Friedl, M., Gao, F., Gorelick, N., Hansen, M., Healey, S., Hostert, P., Hulley,
 733 G., Huntington, J.L., Johnson, D.M., Neigh, C., Lyapustin, A., Lymburner, L.,
 734 Pahlevan, N., Pekel, J.-F., Scambos, T.A., Schaaf, C., Strobl, P., Woodcock,
 735 C.E., Zhang, H.K., Zhu, Z., 2024. Need and vision for global medium-resolution
 736 landsat and sentinel-2 data products. *Remote Sensing of Environment* 300,
 737 113918. <https://doi.org/10.1016/j.rse.2023.113918>
- 738 Razenkova, E., 2023. *Developing remotely sensed indices for biodiversity studies
 739 across the conterminous US* (PhD thesis).
- 740 Razenkova, E., Farwell, L.S., Elsen, P., Carroll, K.A., Pidgeon, A.M., Radeloff,
 741 V., 2022. *Explaining bird richness with the dynamic habitat indices across the
 742 conterminous US* 2022, B15A–05.
- 743 Skidmore, A.K., Coops, N.C., Neinavaz, E., Ali, A., Schaepman, M.E., Paganini,
 744 M., Kissling, W.D., Vihervaara, P., Darvishzadeh, R., Feilhauer, H., Fernan-
 745 dez, M., Fernández, N., Gorelick, N., Geijzendorffer, I., Heiden, U., Heurich,
 746 M., Hoborn, D., Holzwarth, S., Muller-Karger, F.E., Van De Kerchove, R.,
 747 Lausch, A., Leitão, P.J., Lock, M.C., Mücher, C.A., O'Connor, B., Rocchini,
 748 D., Turner, W., Vis, J.K., Wang, T., Wegmann, M., Wingate, V., 2021. Priority
 749 list of biodiversity metrics to observe from space. *Nature Ecology & Evolution*
 750 <https://doi.org/10.1038/s41559-021-01451-x>
- 751 Suttidate, N., Steinmetz, R., Lynam, A.J., Sukmasuang, R., Ngoprasert, D., Chutipong,
 752 W., Bateman, B.L., Jenks, K.E., Baker-Whatton, M., Kitamura, S., Ziolkowska,
 753 E., Radeloff, V.C., 2021. Habitat connectivity for endangered indochinese tigers
 754 in thailand. *Global Ecology and Conservation* 29. <https://doi.org/10.1016/j.gecco.2021.e01718>
- 756 Thomas, C.D., Cameron, A., Green, R.E., Bakkenes, M., Beaumont, L.J., Colling-
 757 ham, Y.C., Erasmus, B.F.N., Siqueira, M.F. de, Grainger, A., Hannah, L.,
 758 Hughes, L., Huntley, B., Jaarsveld, A.S. van, Midgley, G.F., Miles, L., Ortega-
 759 Huerta, M.A., Peterson, A.T., Phillips, O.L., Williams, S.E., 2004. Extinction
 760 risk from climate change. *Nature* 427, 5.
- 761 Thompson, I.D., Mackey, B., McNulty, S., Mosseler, A., 2009. Forest resilience,
 762 biodiversity, and climate change: a synthesis of the biodiversity / resiliende /
 763 stability relationship in forest ecosystems, CBD technical series. Secretariat of
 764 the Convention on Biological Diversity, Montreal.
- 765 Urban, M.C., 2015. Accelerating extinction risk from climate change. *Science* 348,
 766 571–573. <https://doi.org/10.1126/science.aaa4984>
- 767 Valbuena, R., O'Connor, B., Zellweger, F., Simonson, W., Vihervaara, P., Maltamo,
 768 M., Silva, C.A., Almeida, D.R.A., Danks, F., Morsdorf, F., Chirici, G., Lucas,
 769 R., Coomes, D.A., Coops, N.C., 2020. Standardizing ecosystem morphological
 770 traits from 3D information sources. *Trends in Ecology & Evolution* 35, 656–667.
 771 <https://doi.org/10.1016/j.tree.2020.03.006>

- 772 White, Joanne.C., Wulder, M.A., Hobart, G.W., Luther, J.E., Hermosilla, T.,
773 Griffiths, P., Coops, N.C., Hall, R.J., Hostert, P., Dyk, A., Guindon, L., 2014.
774 Pixel-based image compositing for large-area dense time series applications and
775 science. Canadian Journal of Remote Sensing 40, 192212. <https://doi.org/10.1080/07038992.2014.945827>
776 Zhu, Z., Woodcock, C.E., 2012. Object-based cloud and cloud shadow detection
777 in Landsat imagery. Remote Sensing of Environment 118, 83–94. <https://doi.org/10.1016/j.rse.2011.10.028>
779